Biosensors and Bioelectronics 26 (2011) 4791–4797

Contents lists available at ScienceDirect

Biosensors and Bioelectronics

journal homepage: www.elsevier.com/locate/bios

Synthesis of functional SiO_2-coated graphene oxide nanosheets decorated with Ag nanoparticles for H_2O_2 and glucose detection

Wenbo Lu, Yonglan Luo, Guohui Chang, Xuping Sun*

State Key Lab of Electroanalytical Chemistry, Changchun Institute of Applied Chemistry, Chinese Academy of Sciences, Changchun 130022, Jilin, PR China

ARTICLE INFO

Article history:
Received 2 April 2011
Received in revised form 19 May 2011
Accepted 10 June 2011
Available online 17 June 2011

Keywords:
SiO_2
Graphene oxide
Ag nanoparticle
H_2O_2
Glucose

ABSTRACT

In this paper, we report on the first preparation of well-defined SiO_2-coated graphene oxide (GO) nanosheets (SiO_2/GO) without prior GO functionalization by combining sonication with sol–gel technique. The functional SiO_2/GO nanocomposites (F-SiO_2/GO) obtained by surface functionalization with NH_2 group were subsequently employed as a support for loading Ag nanoparticles (AgNPs) to synthesize AgNP-decorated F-SiO_2/GO nanosheets (AgNP/F-SiO_2/GO) by two different routes: (1) direct adsorption of preformed, negatively charged AgNPs; (2) in situ chemical reduction of silver salts. The morphologies of these nanocomposites were characterized by transmission electron microscopy (TEM) and scanning electron microscopy (SEM). It is found that the resultant AgNP/F-SiO_2/GO exhibits remarkable catalytic performance for H_2O_2 reduction. This H_2O_2 sensor has a fast amperometric response time of less than 2 s. The linear range is estimated to be from 1×10^{-4} M to 0.26 M (rY = 0.998) and the detection limit is estimated to be 4×10^{-6} M at a signal-to-noise ratio of 3, respectively. We also fabricated a glucose biosensor by immobilizing glucose oxidase (GOD) into AgNP/F-SiO_2/GO nanocomposite-modified glassy carbon electrode (GCE) for glucose detection. Our study demonstrates that the resultant glucose biosensor can be used for the glucose detection in human blood serum.

1. Introduction

Graphene, a single layer of sp^2-bonded carbon atoms packed into a benzene-ring structure from which graphite, carbon nanotubes (Hu et al., 2010), and fullerenes (Tashiro and Aida, 2007) are derived, has become the subject of high interest in the field of material science (Geim, 2009; Chen et al., 2010; Li and Kaner, 2008). Graphene-based nanocomposites have stimulated intense research over past decades because of their new optical, electronic, mechanical, and catalytic properties (Jin et al., 2010; Yang et al., 2010; Teague et al., 2009; Wu et al., 2007). Particularly, due to the large surface area and above mentioned properties, graphene oxide (GO) has been an attractive choice as the substrate for nanocomposites (Meyer et al., 2007; Zhou et al., 2009). Among them, Ag nanoparticles (AgNPs)/GO nanocomposites have attracted immense attention. Up to now, only limited synthesis approaches including in situ chemical reduction of Ag^+ on GO absorbed on 3-aminopropyltriethoxysilane (APTES)-modified Si/SiOx substrates (Zhou et al., 2009), electrostatic force directed assembly of Ag nanocrystals synthesized from an arc plasma source (Lu et al., 2009) and solution-based single-step chemical synthesis method (Xu and Wang, 2009) have been developed. However, all these above-mentioned methods suffer from more or less drawbacks such as the adsorption of GO on solid substrates (Zhou et al., 2009), the involvement of special equipment (Lu et al., 2009), or the requirement of an extra reducing agent (Xu and Wang, 2009). Accordingly, the development of new preparation strategy overcoming all the shortcomings is highly desired.

On the other hand, H_2O_2 sensor is of great importance in the fields of chemistry, biology, clinical control, and environmental protection (Luo et al., 2004; Shu et al., 2007; Klassen et al., 1994; Jia et al., 2002; Wang et al., 2009). Early H_2O_2 sensors involved the use of intrinsic selectivity and sensitivity of enzymatic reactions where nanostructures are also employed to immobilize the enzymes and at the same time, to reduce the possibility of protein denaturing (Willner and Katz, 2000; Xiao et al., 2003; Song et al., 2006). It has been shown that AgNPs show good catalytic activity toward H_2O_2 reduction (Liu et al., 2010a,b), opening the door for designing of enzymeless H_2O_2 sensors (Liu et al., 2010a,b; Song et al., 2009; Lu et al., 2011). Our group also constructed a AgNPs-based electrochemical H_2O_2 sensor, which exhibited potential application of AgNPs in sensor (Lu et al., 2011). On the other hand, glucose oxidase (GOD) can catalyze the oxidation of glucose to H_2O_2 and gluconolactone in the presence of O_2 where the determination of the glucose is based on monitoring the production of H_2O_2 (Shan et al., 2010; Song et al., 2010; Jia et al., 2010). Therefore, glucose

* Corresponding author. Tel.: +86 431 85262065; fax: +86 431 85262065.
E-mail address: sunxp@ciac.jl.cn (X. Sun).

0956-5663/$ – see front matter © 2011 Elsevier B.V. All rights reserved.
doi:10.1016/j.bios.2011.06.008

detection can be achieved via the determination of H_2O_2 generated by GOD-catalyzed oxidation of glucose.

In this study, we report on the first preparation of AgNP-modified NH_2 functionalized silica-coated GO nanosheets (SiO_2/GO) in solution by two different routes: (1) direct adsorption of preformed, negatively charged AgNPs; (2) in situ chemical reduction of Ag^+. The functional SiO_2/GO nanocomposites (F-SiO_2/GO) were obtained by surface functionalization with ATPES of well-defined SiO_2/GO, which were prepared by depositing SiO_2 without prior GO functionalization by combining sonication with sol–gel technique. It was found that the resultant AgNP/F-SiO_2/GO composites exhibit notable catalytic performance toward H_2O_2 reduction. Furthermore, we demonstrated the construction of glucose biosensor by immobilizing glucose oxidase (GOD) into AgNP/F-SiO_2/GO nanocomposite-modified glassy carbon electrode (GCE) for glucose detection in buffer and human blood serum. To the best of knowledge, it is the first H_2O_2 and glucose sensor with the use of AgNPs/GO nanocomposites as catalysts.

2. Experimental

2.1. Materials

$AgNO_3$, NaH_2PO_4, Na_2HPO_4, APTES, $KMnO_4$, tetraethyl orthosilicate (TEOS), graphite, GOD, glucose, chitosan and H_2O_2 (30 wt%) were purchased from Aladin Ltd. (Shanghai, China). $NaNO_3$, ammonium hydroxide ($NH_3{\cdot}H_2O$) (28 wt% in water), H_2SO_4, sodium citrate, ethanol were purchased from Shanghai Chemical Factory (Shanghai, China). All chemicals were used as received without further purification. The water used throughout all experiments was purified through a Millipore system. Phosphate buffer saline (PBS) was prepared by mixing stock solutions of NaH_2PO_4 and Na_2HPO_4 and a fresh solution of H_2O_2 was prepared daily.

2.2. Instruments

Atomic force microscopy (AFM) was conducted with a SPI3800N microscope (Seiko Instruments, Inc.). Transmission electron microscopy (TEM) measurements were made on a HITACHI H-8100 EM (Hitachi, Tokyo, Japan) with an accelerating applied potential of 200 kV. The sample for TEM characterization was prepared by placing a drop of the dispersion on carbon-coated copper grid and dried at room temperature. Scanning electron microscopy (SEM) measurements were made on a XL30 ESEM FEG scanning electron microscope at an accelerating applied potential of 20 kV. The sample for SEM characterization was prepared by placing a drop of the dispersion on a bare indium tin oxide coated glass substrate (ITO) and air-dried at room temperature. Electrochemical measurements are performed with a CHI 660D electrochemical analyzer (CH Instruments, Inc., Shanghai). A conventional three-electrode cell is used, including a GCE (geometric area = 0.07 cm^2) as the working electrode, a Ag/AgCl (3 M KCl) electrode as the reference electrode, and platinum foil as the counter electrode. All potentials given in this work are referred to the Ag/AgCl electrode. All the experiments are carried out at ambient temperature.

2.3. Preparation of GO

GO was prepared from natural graphite powder through a modified Hummers method (Hummers and Offeman, 1958). In a typical synthesis, 1 g of graphite was added into 23 mL of 98% H_2SO_4, followed by stirring at room temperature over a 24 h period. After that, 100 mg of $NaNO_3$ was introduced into the mixture and stirred for 30 min. Subsequently, the mixture was kept below 5 °C by ice bath, and 3 g of $KMnO_4$ was slowly added into the mixture. After being heated to 35–40 °C, the mixture was stirred for another 30 min. After that, 46 mL of water was added into above mixture during a period of 25 min. Finally, 140 mL of water and 10 mL of 30% H_2O_2 were added into the mixture to stop the reaction. After the unexploited graphite in the resulting mixture was removed by centrifugation, as-synthesized GO was dispersed into individual sheets in distilled water at a concentration of 0.5 mg/mL with the aid of ultrasound for further use.

2.4. Synthesis of F-SiO_2/GO nanosheets

In a typical synthesis, 2.5 mL of GO (0.6 mg/mL) aqueous solution was added into 20 mL of ethanol solution, followed by addition of 1 mL of $NH_3{\cdot}H_2O$. After stirring at room temperature for 5 min, 50 μL of TEOS was added into the mixture. After that, the mixture was sonicated for more than 9 h and kept overnight at room temperature. Then, 30 μL of APTES was added to the above solution, followed by the addition of 0.6 mL of $NH_3{\cdot}H_2O$. The resulting mixture was stirred for more than 12 h. Finally, the product was centrifuged (removing the excess APTES) and further washed with ethanol and water three times, respectively. The resulting precipitates were redispersed in 5 mL of water for characterization and further use.

2.5. Preparation of AgNPs

AgNPs were prepared via reduction of $AgNO_3$ by sodium citrate, according to established method (Lee and Meisel, 1982). In brief, 16 μL of 0.5 M $AgNO_3$ aqueous solution was introduced into 10 mL of 1% sodium citrate solution under stirring. Then the resulting mixture was heated to 100 °C and kept at this temperature for 60 min. As-formed AgNPs dispersion was stored at 4 °C for further use.

2.6. Preparation of AgNP-decorated F-SiO_2/GO nanocomposites

In the present study, two different methods were used to prepare AgNP/F-SiO_2/GO nanocomposites. (1) The nanocomposites were prepared by adsorption of citrate-stabilized AgNPs onto the F-SiO_2/GO nanosheets (designated as AgNP-A/F-SiO_2/GO). The AgNP-A/F-SiO_2/GO nanocomposites were prepared via mixing 300 μL of F-SiO_2/GO dispersion aqueous solution into 1.5 mL of AgNPs aqueous solutions (slight excess) first, and then the mixture was sonicated for 30 min. After that, the mixture was placed at room temperature over a period of 1 h. Finally, the precipitate was collected by centrifugation and washed with water twice and then redispersed in 0.1 mL of water for characterization and further use. (2) The nanocomposites were prepared by in situ reduction of $AgNO_3$ onto the F-SiO_2/GO nanosheets (designed as AgNP-R/F-SiO_2/GO). In a typical synthesis, 20 μL of 0.5 M $AgNO_3$ was added into 1 mL of F-SiO_2/GO nanosheets dispersion first, and then the mixture was heated at 100 °C over a period of 60 min. The precipitate was collected by centrifugation and washed with water twice. Then, the resultant products were redispersed in 0.3 mL of H_2O for characterization and further use.

2.7. Preparation of GOD/AgNP-A/F-SiO_2/GO composites

100 μL of F-SiO_2/GO dispersion was added to 1 mL 0.5% chitosan solution containing 30 mg GOD and 1 mL of AgNPs dispersion first, after that, the mixture was placed at 4 °C over a period of 8 h. Then, the GOD/AgNP-A/F-SiO_2/GO composites were collected by centrifugation.

2.8. Electrocatalytic experiments

The modified electrodes were prepared by a simple casting method. Prior to the surface coating, the GCE was polished

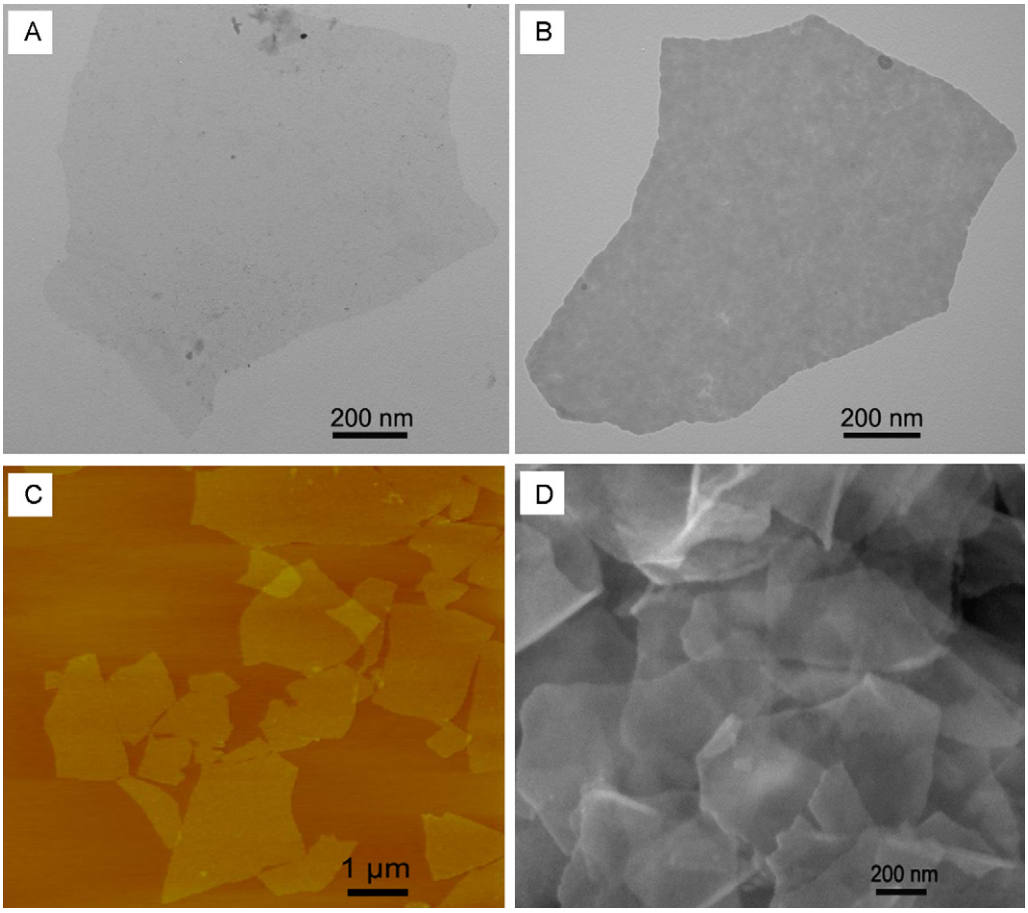

Fig. 1. Typical TEM images of (A) GO nanosheets and (B) F-SiO_2/GO nanosheets, (C) atomic force microscopy (AFM) images of GO nanosheets, and (D) SEM image of F-SiO_2/GO nanosheets.

with 1.0 and 0.3 μm alumina powder, respectively, and rinsed with doubly distilled water, followed by sonication in ethanol solution and doubly distilled water successively. Then, the electrode was allowed to dry in a stream of nitrogen. For the cyclic voltammetry experiment, 4 μL of AgNP/F-SiO_2/GO composites was dropped on the surface of pretreated GCE and left to dry at room temperature. The GOD/AgNP-A/F-SiO_2/GO composites modified GCE (GOD/AgNP-A/F-SiO_2/GO/GCE) was similar prepared. Exceptionally, the GOD/AgNP-A/F-SiO_2/GO/GCE was let to dry at 4 °C for 2.5 h. For current time experiment, 2 μL of Nafion (0.2%) was additionally cast on the surface of the above modified GCE and dried before electrochemical experiments.

3. Results and discussion

3.1. Characterization of AgNP-decorated F-SiO_2/GO composites

Fig. 1A shows typical TEM image of the as-made GO nanosheets. It is obviously seen that the GO sheet is about 1.5 μm in width. A number of GO nanosheets are shown in Fig. 1C, indicating the successful preparation of GO by Hummers method (Hummers and Offeman, 1958). The GO sheets range from approximately 1 μm to 3 μm in lateral dimensions, as shown in Fig. 1C. The GO sheet is about 1.15 nm in thickness is observed in the AFM image (Balamurugan and Chen, 2009; Lian et al., 2009; Fig. S1). Fig. 1B shows the TEM image of the F-SiO_2/GO nanosheets, revealing that very homogeneous silica layers are coated on the surface of GO nanosheet. It is clearly seen that the F-SiO_2/GO nanosheet exhibits much deeper color than GO in the same background color, indicating that the F-SiO_2/GO nanosheets are formed. Fig. 1D shows the typical SEM image of the F-SiO_2/GO nanosheets. The morphologies of F-SiO_2/GO nanosheets are shown in Fig. 1D. All above observations indicate that the F-SiO_2/GO nanosheets are formed successfully.

APTES protonates and thus is positively charged at neutral pH. Given that citrate-stabilized AgNPs are negatively charged, it is expected that the resultant F-SiO_2/GO can be easily decorated with AgNPs via direct adsorption of performed, negatively charged, citrate-stabilized AgNPs. Fig. 2A shows typical SEM image of the products formed by incubating F-SiO_2/GO nanosheets with citrate-stabilized AgNPs over a period of 1 h, indicating that a large amount of nanoparticles (white dots) are adsorbed on the nanosheet. Such observation is also evidenced by the high magnification image, as shown in Fig. 2B. It is clearly seen that these nanoparticles on the F-SiO_2/GO sheets are spherical in shape and range from 10 to 30 nm. The chemical composition of the material was further determined by the corresponding energy-dispersive spectrum (EDS) (Fig. S2). An intensive peak of Ag element is observed, suggesting these particles on the sheets are AgNPs. Because $-NH_2$ groups can reduce Ag^+ into metallic Ag (Zhou et al., 2009; Liu et al., 2010a,b), we further explored feasibility of in situ reduction of Ag^+ onto F-SiO_2/GO nanosheets. Fig. S3 shows the typical TEM images of products thus formed. It is clearly seen that the in situ chemical reduction method successfully results in the formation of small AgNPs on the F-SiO_2/GO surfaces, as shown in Fig. S3A. The corresponding high magnification image (Fig. S3B) further confirms the formation of AgNPs on F-SiO_2/GO. A schematic (not to scale) to illustrate the

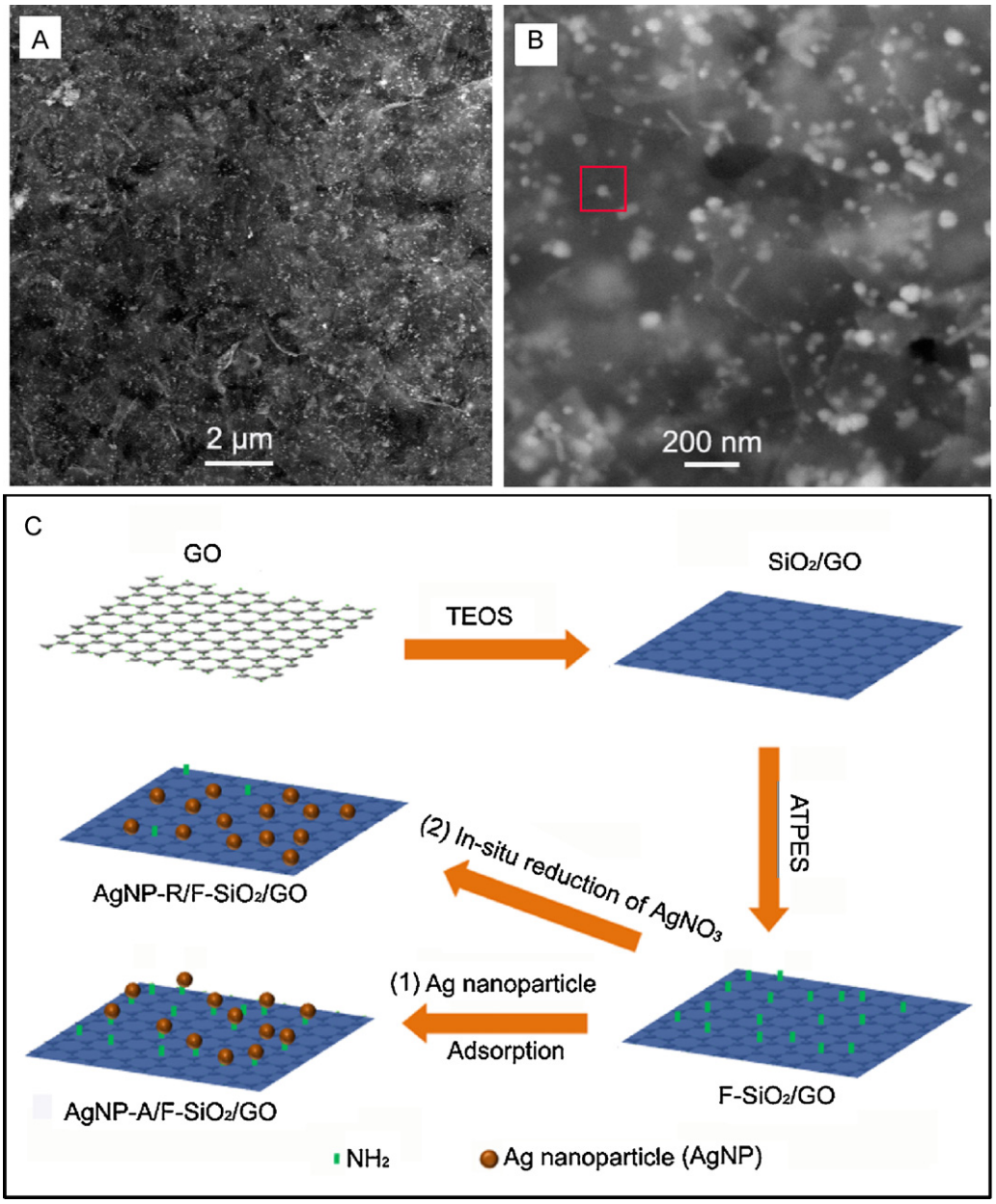

Fig. 2. (A) Low and (B) high mgnification SEM images of the AgNP-A/F-SiO_2/GO nanocomposites, and (C) a schematic (not to scale) to illustrate the formation procedure of AgNP-A/F-SiO_2/GO and AgNP-R/F-SiO_2/GO nanosheets.

formation procedure of AgNP/F-SiO_2/GO nanosheets is shown in Fig. 2C.

3.2. Cyclic voltammograms of H_2O_2 sensor

To testify the sensing application of the AgNP/F-SiO_2/GO nanocomposites, we designed an enzymeless H_2O_2 sensor by direct deposition of the AgNP-A/F-SiO_2/GO composites on a bare GCE surface. Fig. 3 shows the electrocatalytic responses of bare GCE, F-SiO_2/GO nanosheets modified GCE (F-SiO_2/GO/GCE), AgNP-A/F-SiO_2/GO nanocomposites modified GCE (AgNP-A/F-SiO_2/GO/GCE) and AgNP-R/F-SiO_2/GO nanocomposites modified GCE (AgNP-R/F-SiO_2/GO/GCE) toward the reduction of H_2O_2 in 0.2 M PBS at pH 6.5 in the presence of 1×10^{-3} M H_2O_2. It is obviously seen that the responses of both the bare GCE and F-SiO_2/GO/GCE toward the reduction of H_2O_2 are quite weak. In contrast, the AgNP-A/F-SiO_2/GO/GCE exhibits a remarkable catalytic current peak about 25 μA in intensity at −0.58 V vs. Ag/AgCl. It is also important to note that the AgNP-A/F-SiO_2/GO/GCE exhibits no electrochemical response in the absence of H_2O_2. All the above observations indicate that the AgNPs contained in the nanocomposites exhibit a notable catalytic performance for H_2O_2 reduction and the GO exhibits no catalytic activity. Although the edge plane sites have been reported to be key to graphene/GO (Kampouris and Banks, 2010; Hallam and Banks, 2011), the reason for our failure to observe the catalytic activity of GO in our present study could be that the GO nanosheet is completely coated by SiO_2. Compared to GCE modified by simple electroreduction of Ag^+ (Cui et al., 2008) and a Pt electrode decorated with Ag nanoparticles in polyvinyl alcohol film (Guascito et al., 2008), the AgNP-A/F-SiO_2/GO/GCE exhibits the 66.6% and 38.8% enhancement of peak current, respectively. Meanwhile, it exhibits a 240 mV and 80 mV positive shift of the peak potential compared to AgNP-modified GCE by electrodeposition technique (Welch et al., 2005) and hydrothermal synthesis of PQ11-AgNPs

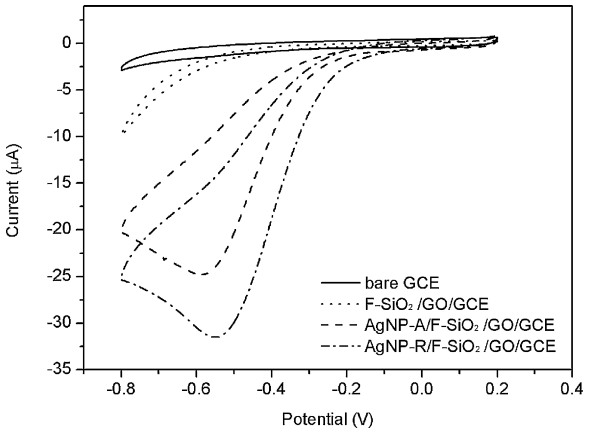

Fig. 3. Cyclic voltammograms (CVs) of bare GCE, F-SiO_2/GO/GCE, AgNP-A/F-SiO_2/GO/GCE and AgNP-R/F-SiO_2/GO/GCE in N_2-saturated 0.2 M PBS at pH: 6.5 in the presence of 1×10^{-3} M H_2O_2 (scan rate: 50 mV/s).

decorated GCE (Lu et al., 2011), respectively. In addition, the relative standard deviation (RSD) of the amperometric response to 1×10^{-3} M H_2O_2 was 4.3% for 10 successive measurements, indicating the good reproducibility of the AgNP-A/F-SiO_2/GO/GCE. The stability of the sensor was tested by measuring response currents of the electrode. After 5 days, only 7.1% signal of current was lost, indicating the good stability for H_2O_2 detection. We further compared the responses of AgNP-A/F-SiO_2/GO/GCE with AgNP-R/F-SiO_2/GO/GCE and found that the latter exhibits a 36% enhancement of peak current and a 40 mV positive shift of the peak potential and thus exhibits better catalytic performance. Although the AgNP-R/F-SiO_2/GO/GCE exhibits better catalytic performance, we still choose the AgNP-A/F-SiO_2/GO/GCE in our present study for all measurements, due to its simple preparation process, material saving and sufficient response signal obtained in practical analysis.

3.3. Chronoamperometric response of H_2O_2 sensor

Fig. 4 shows typical current–time plot of the AgNP-A/F-SiO_2/GO/GCE in N_2-saturated 0.2 M PBS buffer (pH: 6.5) on consecutive step change of H_2O_2 concentrations. Although the AgNP-A/F-SiO_2/GO/GCE exhibited the biggest response signal at −0.58 V, determination of the H_2O_2 was carried out at −0.3 V. Such

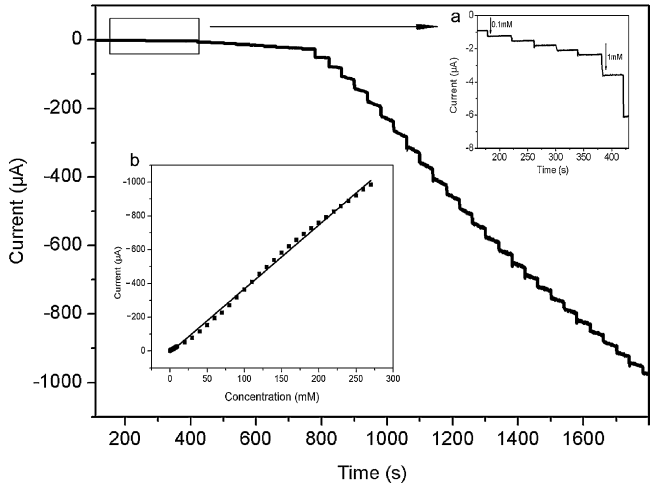

Fig. 4. Typical steady-state response of the AgNP-A/F-SiO_2/GO/GCE to successive injection of H_2O_2 into the stirred N_2-saturated 0.2 M PBS at pH: 6.5. Inset: (a) amplified response curve at low concentrations and (b) the corresponding calibration curve (applied potential: −0.3 V).

a low applied potential can ensure sufficient current response with lower background or less interference of other electroactive species in the solution (Zhao et al., 2009a,b). When an aliquot of H_2O_2 was dropped into the stirring PBS solution, the reduction current rose steeply to reach a stable value. The sensor could accomplish 96% of the steady state current within 3 s, indicating a fast amperometric response behavior. It is apparently seen that the steps shown in Fig. 4 are more horizontal in the region of lower concentration of H_2O_2 and the noises become higher with increased concentration of H_2O_2. Inset b (Fig. 4) shows the calibration curve of the sensor. The linear detection range is estimated to be from 1×10^{-4} M to 0.26 M (rY= 0.998), and the detection limit is estimated to be 4×10^{-6} M at a signal-to-noise ratio of 3. Compared to our previous work, the H_2O_2 sensor herein has improved the detection limit and the linear range. Moreover, the detailed comparison of our present work with others regarding the performance of H_2O_2 assays is presented in Table S1.

3.4. Direct electrochemistry of glucose oxidase

Fig. S4 shows CVs of bare GCE, AgNP-A/F-SiO_2/GO/GCE and GOD/AgNP-A/F-SiO_2/GO/GCE in N_2-saturated PBS solution. It is found that no peak is observed for bare GCE and AgNP-A/F-SiO_2/GO/GCE. The current of bare GCE is higher than that of the AgNP-A/F-SiO_2/GO/GCE, due to the AgNP-A/F-SiO_2/GO/GCE film prevent the GCE surface from the solution. In contrast, the GOD/AgNP-A/F-SiO_2/GO/GCE exhibits a clear electrochemical response. A pair of redox peaks at GOD/AgNP-A/F-SiO_2/GO/GCE is observed (Fig. S4 solid). The anodic peak potential (E_{pa}) is at −0.44 V and cathodic peak potential (E_{pc}) is at −0.37 V. The peak potential separation (ΔE_p) is almost 70 mV. Compared to the CV curve of the AgNP-A/F-SiO_2/GO/GCE, the well-defined redox peaks should be ascribed only to GOD, which is characteristic of reversible electron transfer process of redox active center in the GOD (Shan et al., 2009). All these observations indicate that the GOD still retains its bioactivity after adsorption on the AgNP-A/F-SiO_2/GO nanocomposites.

3.5. Detection of glucose at the GOD/AgNP-A/F-SiO_2/GO-decorated electrode

It is well known that diabetes mellitus is a worldwide public health problem and thus the detection of glucose is of particular importance (Toghill and Compton, 2010). GOD has been the most frequently used glucose recognition element, due to its high binding specificity, high turnover rate and relatively high stability. GOD can selectively catalyze the oxidation of glucose in the presence of oxygen to form H_2O_2, which can be electrochemically detected (Jia et al., 2010; Tsai and Tsai, 2009). The reactions can be described in Fig. S5. To testify the sensing application of the GOD/AgNP-A/F-SiO_2/GO composites, we designed a glucose biosensor by direct deposition of the GOD/AgNP-A/F-SiO_2/GO composites on a bare GCE surface. Fig. 5A shows the electrocatalytic responses of the GOD/AgNP-A/F-SiO_2/GO/GCE in 0.2 M PBS at pH: 7.4 in the presence of 2×10^{-3} M glucose solution. In the beginning, it is obviously seen that two reduction peaks can be observed in Fig. 5A (line a). The peak at −0.44 V vs. Ag/AgCl should consider as the electrode toward the reduction of GOD and the peak at −0.62 V is the reduction of H_2O_2. These observations indicate that GOD/AgNP-A/F-SiO_2/GO/GCE exhibits good electrocatalysis toward the reduction of H_2O_2. A small amount of H_2O_2 in the solution generated by the GOD catalyzes the oxidation of glucose in the beginning of the reaction. With increasing the number of scan cycle to 2, the reduction peak of GOD changes weaker and the reduction peak of H_2O_2 becomes stronger, as shown in Fig. 5A (line b). A further increase the number of scan cycle to 3, the peak reduction of

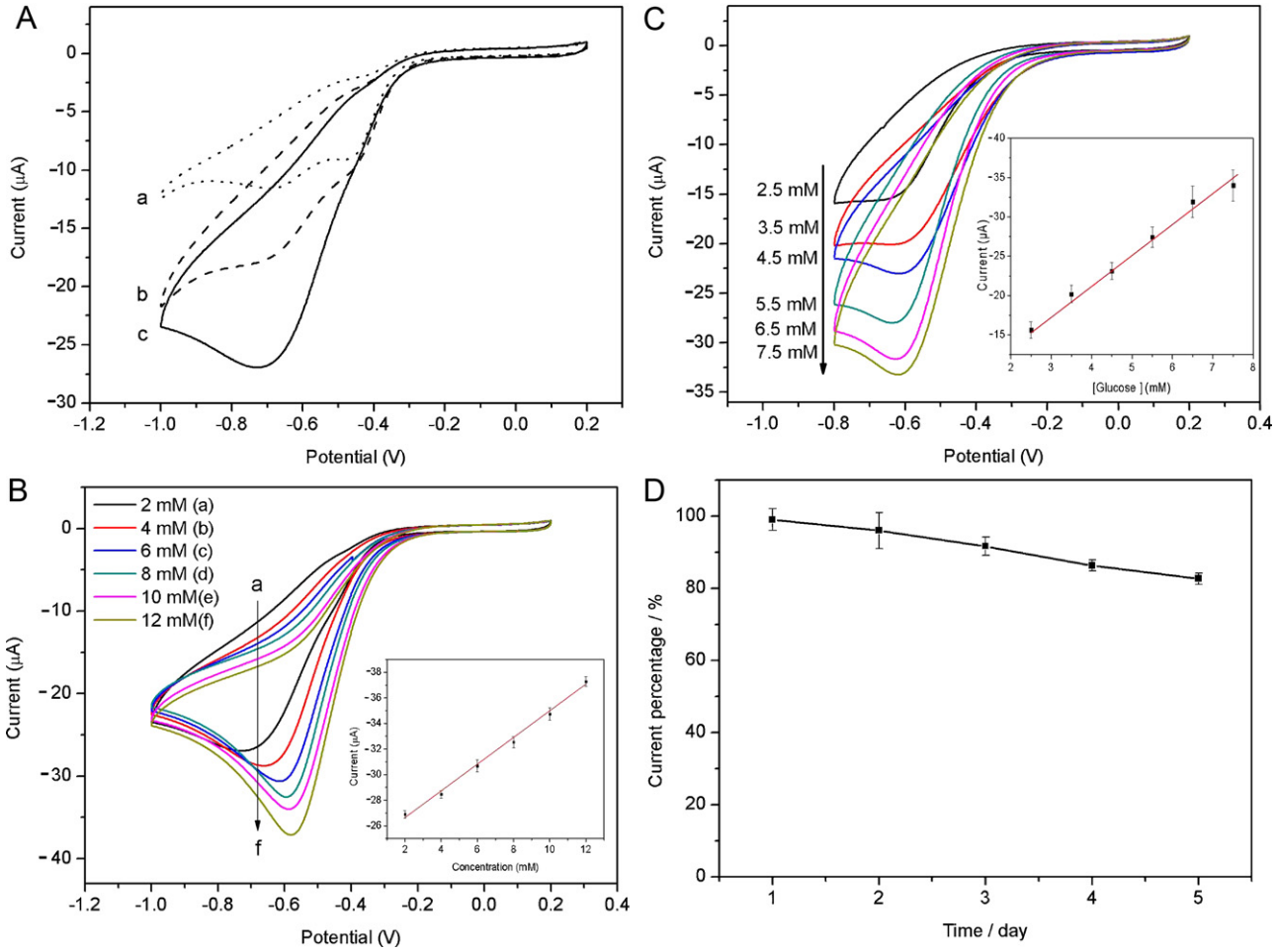

Fig. 5. (A) CVs of the GOD/AgNP-A/F-SiO_2/GO/GCE in 0.2 M PBS solution (pH: 7.4) saturated with O_2 in the presence of 2×10^{-3} M glucose solution. Line a: the 1st scan cycle, line b: the 2nd scan cycle, and line c: the 3rd scan cycle. (B) CVs of the GOD/AgNP-A/F-SiO_2/GO/GCE in PBS solution (pH: 7.4) in the presence of various concentrations of glucose saturated with O_2: 2, 4, 6, 8, 10 and 12 mM from inner to outer. Inset is the calibration curve (R = 0.996) corresponding to amperometric responses at the reduction peak. (C) CVs of the GOD/AgNP-A/F-SiO_2/GO/GCE in real blood serum sample and PBS solution (pH: 7.4) in the presence of various concentrations of glucose saturated with O_2: 2.5, 3.5, 4.5, 5.5, 6.5 and 7.5 mM from inner to outer. Inset is the calibration curve (R = 0.993) corresponding to amperometric responses at the reduction peak. (D) The variation in the response current of 3 mM glucose in PBS solution (pH: 7.4) at the GOD/AgNP-A/F-SiO_2/GO/GCE for 5 days. Scan rate: 50 mV/s.

GOD could not be observed, because the peak of reduction of H_2O_2 is very strong (Fig. 5A, line c). All these observations indicate that the GOD/AgNP-A/F-SiO_2/GO/GCE can detect glucose via that the GOD catalyzes the oxidation of glucose to generate H_2O_2 which is subsequently detected electrochemically by AgNP-catalyzed reduction of H_2O_2. Fig. 5B shows CVs of the GOD/AgNP-A/F-SiO_2/GO/GCE in PBS solution (pH: 7.4) in present of various concentrations of glucose saturated with O_2. The signal responses of the GOD/AgNP-A/F-SiO_2/GO/GCE on glucose with different concentrations were recorded in the solution of 0.2 M PBS (pH: 7.4) via increasing glucose concentration step by step. When the concentration of glucose increases from 2 mM to 12 mM, the amount of H_2O_2 which generated by the GOD catalyzes the oxidation of glucose increase quickly, and the current of H_2O_2 reduction peaks (Fig. 5A) at about −0.62 V presents a continuous enhancement, as shown in Fig. 5B. The inset of Fig. 5B shows the catalytic current versus glucose concentration relationship. A good linear relationship is found between the catalytic current and glucose concentration at a range from 2 to 12 mM (R = 0.996). The detection limit of glucose is 310 μm. The relative standard deviation (RSD) of the current response to 8 mM glucose is 4.1% for 5 successive measurements, indicating that the glucose biosensor has good reproducibility. Compared to the RSD of the PtNPs based glucose biosensor is 5.2% (Kang et al., 2008), the biosensor designed here has better reproducibility. Since the blood glucose levels of normal persons are between 2 and 10 mM (Shan et al., 2010), the linear response from 2 to 12 mM of the glucose biosensor offers a way for glucose detection in normal persons' blood serum.

3.6. Real sample analysis and stability of glucose biosensor

To testify the feasibility of the GOD/AgNP-A/F-SiO_2/GO/GCE in practical analysis, we employed the biosensor to measure glucose in human blood serum. The original glucose concentration of the human blood sample is hypothesized as 6 mM. The electrolyte solution containing 1.5 mL of the serum sample and 3.5 mL phosphate buffer solution (pH: 7.4) is used for CV experiment. The reduction peak current increases with successive addition of 1 mM glucose into the blood serum saturated with O_2, as shown in Fig. 5C. The inset of Fig. 5C shows that the peak currents increase linearly with increasing the glucose concentrations saturated with O_2 (R = 0.993). The RSD of the current response to 6.5 mM glucose is 4.5% for 5 successive measurements. All the above observations indicate that the biosensor offers a method to detect glucose in human blood serum.

The long-term stability of the prepared glucose biosensor is a critical factor in practical application. To evaluate the stability of the glucose biosensor, the GOD/AgNP-A/F-SiO_2/GO/GCE was stored at 4 °C when not in use. The stability was examined by periodical

measurements of the biosensor responses to 3 mM glucose in PBS solution (pH: 7.4) at a scan rate of 50 mV/s. The variation of the response current at the GOD/AgNP-A/F-SiO_2/GO/GCE decreased to about 95% of its initial response current on the 2nd day and about 83% on the 5th day, as shown in Fig. 5D. The loss of the response current may ascribe to the decrease of the enzyme activity during these days.

4. Conclusions

In summary, we have demonstrated a simple method for the synthesis of well-defined SiO_2/GO nanosheets and their subsequent use as an advanced support for loading AgNPs via direct adsorption of preformed, negatively charged AgNPs and in situ chemical reduction of silver salts. The detection of H_2O_2 without using enzyme in the electrode modified by AgNP/F-SiO_2/GO nanocomposites has also been demonstrated. Furthermore, a glucose biosensor has also been constructed via immobilizing GOD into the nanocomposite-modified GCE. Such AgNP/F-SiO_2/GO nanocomposites may hold great promise for applications in areas including biosensor, analytical and electroanalytical chemistry.

Appendix A. Supplementary data

Supplementary data associated with this article can be found, in the online version, at doi:10.1016/j.bios.2011.06.008.

References

Balamurugan, A., Chen, S., 2009. Electroanalysis 21, 1419–1423.
Chen, D., Tang, L., Li, J., 2010. Chem. Soc. Rev. 39, 3157–3180.
Cui, K., Song, Y., Yao, Y., Huang, Z., Wang, L., 2008. Electrochem. Commun. 10, 663–667.
Geim, A.K., 2009. Science 324, 1530–1534.
Guascito, M.R., Filippo, E., Malitesta, C., Manno, D., Serra, A., Turco, A., 2008. Biosens. Bioelectron. 24, 1057–1063.
Hallam, P.M., Banks, C.E., 2011. Electrochem. Commun. 13, 8–11.
Hu, L., Hecht, D.S., Gruner, G., 2010. Chem. Rev. 110, 5790–5844.
Hummers Jr., W.S., Offeman, R., 1958. J. Am. Chem. Soc. 80, 1339–11339.
Jia, J., Wang, B., Wu, A., Cheng, G., Li, Z., Dong, S., 2002. Anal. Chem. 74, 2217–2223.
Jia, W., Wang, K., Xia, X., 2010. Trends Anal. Chem. 29, 306–318.
Jin, E., Lu, X., Cui, L., Chao, D., Wang, C., 2010. Electrochim. Acta 55, 7230–7234.
Kampouris, D.K., Banks, C.E., 2010. Chem. Commun. 46, 8986–8988.
Kang, X., Mai, Z., Zou, X., Cai, P., Mo, J., 2008. Talanta 74, 879–886.
Klassen, N.V., Marchington, D., McGovan, H.C.E., 1994. Anal. Chem. 66, 2921–2925.
Lee, P.C., Meisel, D., 1982. J. Phys. Chem. 86, 3391–3395.
Lian, W., Wang, L., Song, Y., Yuan, H., Zhao, S., Li, P., Chen, L., 2009. Electrochim. Acta 54, 4334–4339.
Li, D., Kaner, R.B., 2008. Science 320, 1170–1171.
Lin, D., Jiang, Y., Wang, Y., Sun, S., 2008. J. Nanomater. 1, 473791–473801.
Liu, A., Dong, W., Liu, E., Tang, W., Zhu, J., Han, J., 2010a. Electrochim. Acta 55, 1971–1974.
Liu, S., Tian, J., Wang, L., Li, H., Zhang, Y., Sun, X., 2010b. Macromolecules 43, 10078–10083.
Luo, X., Xu, J., Zhao, W., Chen, H., 2004. Biosens. Bioelectron. 19, 1295–1300.
Lu, G., Mao, S., Park, S., Ruoff, R.S., Chen, J., 2009. Nano Res. 2, 192–200.
Lu, W., Liao, F., Luo, Y., Chang, G., Sun, X., 2011. Electrochim. Acta 56, 2295–2298.
Meyer, J.C., Geim, A.K., Katsnelson, M.I., Novoselov, K.S., Booth, T.J., Roth, S., 2007. Nature 446, 60–63.
Shan, C., Yang, H., Song, J., Han, D., Ivaska, A., Niu, L., 2009. Anal. Chem. 81, 2387–2391.
Shan, C., Yang, H., Han, D., Zhang, Q., Ivaska, A., Niu, L., 2010. Biosens. Bioelectron. 25, 1070–1074.
Shu, X., Chen, Y., Yuan, H., Gao, S., Xiao, D., 2007. Anal. Chem. 79, 3695–3702.
Song, Y., Cui, K., Wang, L., Chen, S., 2009. Nanotechnology 20, 105501–105508.
Song, Y., Qu, K., Zhao, C., Ren, J., Qu, X., 2010. Adv. Mater. 22, 2206–2210.
Song, Y., Wang, L., Ren, C., Zhu, G., Li, Z., 2006. Sens. Actuators B 114, 1001–1006.
Tashiro, K., Aida, T., 2007. Chem. Soc. Rev. 36, 189–197.
Teague, M.L., Lai, A.P., Velasco, J., Hughes, C.R., Beyer, A.D., Bockrath, M.W., Lau, C.N., Yeh, N.C., 2009. Nano Lett. 9, 2542–2546.
Toghill, K.E., Compton, R.G., 2010. Int. J. Electrochem. Sci. 5, 1246–1301.
Tsai, M., Tsai, Y., 2009. Sens. Actuators B 141, 592–598.
Wang, B., Zhang, J., Pan, Z., Tao, X., Wang, H., 2009. Biosens. Bioelectron. 24, 1141–1145.
Welch, C., Banks, C., Simm, A., Compton, R., 2005. Anal. Bioanal. Chem. 382, 12–21.
Willner, I., Katz, E., 2000. Angew. Chem. Int. Ed. 39, 1180–1218.
Wu, J., Pisula, W., Mullen, K., 2007. Chem. Rev. 107, 718–743.
Xiao, Y., Patolsky, F., Katz, E., Hainfeld, J., Willner, I., 2003. Science 299, 1877–1881.
Xu, C., Wang, X., 2009. Small 5, 2212–2217.
Yang, S., Feng, X., Wang, L., Tang, K., Maier, J., Mullen, K., 2010. Agrew. Chem. Int. Ed. 49, 4795–4799.
Zhao, B., Liu, Z., Liu, Z., Liu, G., Li, Z., Wang, J., Dong, X., 2009a. Electrochem. Commun. 11, 1707–1712.
Zhao, W., Wang, H., Qin, X., Wang, X., Zhao, Z., Miao, Z., Chen, L., Shan, M., Fang, Y., Chen, Q., 2009b. Talanta 80, 1029–1033.
Zhou, X., Huang, X., Qi, X., Wu, S., Xue, C., Boey, F.Y.C., Yan, Q., Chen, P., Zhang, H., 2009. J. Phys. Chem. C 113, 10842–10846.